

# Rational Design of Allosteric Inhibitors and Activators Using the Population-Shift Model: In Vitro Validation and Application to an Artificial Biosensor

Francesco Ricci,<sup>†,‡,#</sup> Alexis Vallée-Bélisle,<sup>§,||,#,¶</sup> Alessandro Porchetta,<sup>†,‡</sup> and Kevin W. Plaxco<sup>\*,§,||,⊥</sup>

<sup>†</sup>Dipartimento di Scienze e Tecnologie Chimiche, University of Rome, Tor Vergata, Via della Ricerca Scientifica, 00133 Rome, Italy

<sup>‡</sup>Consorzio Interuniversitario Biostrutture e Biosistemi “INBB”, Rome, Italy

<sup>§</sup>Department of Chemistry and Biochemistry, <sup>||</sup>Center for Bioengineering, and <sup>⊥</sup>Interdepartmental Program in Biomolecular Science and Engineering, University of California, Santa Barbara, California 93106, United States

## Supporting Information

**ABSTRACT:** The population-shift mechanism can be used for rational re-engineering of structure-switching biosensors to enable their allosteric inhibition and activation. As a proof-of-principle example of this, we have introduced distal allosteric sites into molecular beacons, which are optical sensors for the detection of specific nucleic acid sequences. The binding of inhibitors and activators to these sites enabled the rational modulation of the sensor's target affinity—and thus its useful dynamic range—over 3 orders of magnitude. The convenience with which this was done suggests that the population-shift mechanism may prove to be a useful method by which allosteric regulation can be introduced into biosensors, “smart” biomaterials, and other artificial biotechnologies.

Allostery, called “the second secret of life” by Perutz,<sup>1</sup> is the primary strategy employed in nature to regulate the affinities of biomolecules and, through this, to control cellular processes and pathways.<sup>2</sup> The ubiquity with which nature employs this mechanism suggests that the ability to engineer allostery into artificial systems could improve the functionality of biomolecules employed in biotechnologies, including synthetic biology,<sup>3</sup> “smart” biomaterials,<sup>4</sup> and biosensors.<sup>5</sup> Motivated by the above arguments, recent work has provided numerous examples in which rational design or directed evolution has been employed to introduce allosteric regulation into normally unregulated enzymes and nucleic acid catalysts (e.g., see refs 6–9). To date, however, the literature has seen little exploration regarding the use of allostery to “tune” the useful dynamic range (the range over which the measurement precision and specificity are optimal) of the receptors used in biosensing applications. In response, we demonstrate here the utility of employing allostery to control the affinity (and thus the dynamic range) of receptors that employ binding-induced conformational changes as a signal transduction mechanism.

A fundamental problem in the fabrication of useful biosensors has been the limited number of biomolecules that produce any readily detectable physical event (e.g., emission of photons or electrons) upon binding to their target. A recent solution to this problem has been the development of a broad

class of biosensors in which target binding is coupled with a large-scale conformational change in the receptor that in turn is transduced into an easily measurable optical, catalytic, or electrochemical output (for a review, see ref 10). Because these sensors are not “spoofed” by nonspecific adsorption of interfering proteins, they tend to work well even in complex sample matrices, such as undiluted blood serum. Moreover, since they are reagentless and rapidly reversible, they support continuous, real-time monitoring (for a review, see ref 11). Finally, because the binding of these receptors is coupled with an unfavorable conformational change, it is possible to tune their affinities by altering the equilibrium constant for this conformational switch.<sup>12</sup> Indeed, by exploiting this population-shift mechanism<sup>13</sup> we were able to tune the affinities of optical biosensors over as much as 5 orders of magnitude via mutations that affect their switching equilibria but leave their specificities unchanged.<sup>12,14</sup> Here, in contrast, we demonstrate the utility of perturbing the conformational switching equilibrium constant—and thus tuning the useful dynamic range—of a structure-switching biosensor via allosteric regulation, which, unlike mutational approaches, renders it possible to modulate the dynamic range “on the fly”, long after its design and fabrication (Figure 1).

As a proof-of-principle demonstration of the allosteric “tuning” of structure-switching biosensors, we have engineered this property into molecular beacons, an optical approach for the detection of specific nucleic acid sequences that is broadly representative of sensors in this class.<sup>12,15</sup> Molecular beacons comprise a single-stranded fluorophore-and-quencher-modified DNA sequence with self-complementary ends. In the absence of the target, the molecular beacon adopts a stem-loop configuration that holds its fluorophore/quencher pair in proximity, suppressing emission. Hybridization of a specific target DNA to the loop breaks the stem and separates the fluorophore/quencher pair, increasing the fluorescence. We have previously shown that, as described by the population-shift model,<sup>13</sup> the affinity with which a molecular beacon binds its target depends quantitatively on both the intrinsic affinity with which the “open” (linear, stem-broken) state binds its cognate target and on the equilibrium constant for the formation of this

Received: May 14, 2012

Published: August 27, 2012

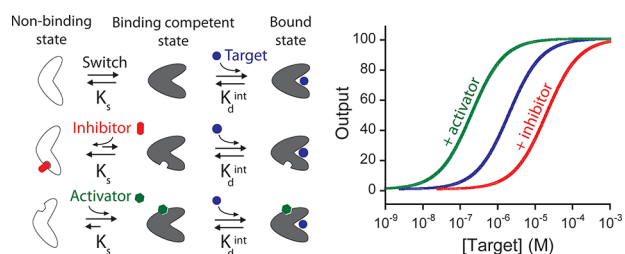


**Figure 1.** Schematic representations of allosterically regulated receptors employing the population-shift mechanism. (top) In this mechanism, target binding shifts a pre-existing equilibrium between a binding-competent state and a nonbinding state.<sup>12,13</sup> Because of this, the overall affinity of the receptor for its target is a function of both the intrinsic affinity of the binding-competent state ( $K_d^{\text{int}}$ ) and the switching equilibrium constant ( $K_s$ ). (middle) The binding of an allosteric inhibitor stabilizes the nonbinding state, reducing  $K_s$  and thus raising the observed dissociation constant. (bottom) The binding of an activator, in contrast, stabilizes the binding-competent state, increasing the target affinity and pushing the dynamic range to lower target concentrations.

state from the “closed,” nonbinding stem–loop configuration.<sup>12</sup> In keeping with this, mutations that affect the stability of the stem and thus alter the conformational switching equilibrium constant ( $K_s$ ) enable rational variation of the beacon’s affinity for its target by many orders of magnitude.

The correlation between a switch-based sensor’s  $K_s$  and the overall affinity with which it binds its target provides a ready route to allosteric inhibition of the sensor. To achieve this, we modified a traditional stem–loop molecular beacon by introducing two single-stranded “tails” acting together as a single allosteric binding site (Figure 2, top). The inhibitor, a single-stranded DNA that binds both tails simultaneously, spans the junction and thus hinders stem opening. The resultant stabilization of the closed stem–loop configuration reduces  $K_s$ ,

which in turn reduces the beacon’s affinity for its target. Consistent with this, as we increased the concentration of the inhibitor from 0 to 3  $\mu\text{M}$ , the affinity of our test-bed molecular beacon decreased, as shown by the monotonic increase in the dissociation constant ( $K_d$ ) from 0.097 to 4.6  $\mu\text{M}$  (Figure 2, bottom).

The behavior of the inhibited molecular beacon is well-described by the population-shift model.<sup>13</sup> To demonstrate this, we start with the Langmuir isotherm, which defines the target concentration/receptor occupancy curve for single-site binding at equilibrium:

$$F_{[T]} = F_0 + \frac{[T](F_B - F_0)}{[T] + K_d} \quad (1)$$

where  $F_{[T]}$  represents the output of the molecular beacon as a function of the target concentration  $[T]$ ,  $F_0$  and  $F_B$  represent the fluorescence intensities of the unbound and target-bound states, respectively, and  $K_d$  is the dissociation constant of the beacon/target duplex. Because of the binding-induced conformational change mechanism of molecular beacons, their affinity is described by the population-shift model,<sup>12</sup> in which  $K_d$  is given by:

$$K_d = K_d^{\text{int}} \left( \frac{1 + K_s}{K_s} \right) \quad (2)$$

where  $K_s$  is the equilibrium constant for switching between the receptor’s nonbinding (closed) and binding-competent (open, linear) states and  $K_d^{\text{int}}$  is the intrinsic affinity of the target for the open state. We previously fabricated molecular beacons with variant stem sequences, thus altering  $K_s$  and in turn tuning the sensor’s useful dynamic range.<sup>12</sup> Here, where we instead modulate the conformational equilibrium via the binding of an allosteric inhibitor,  $K_s$  is given by:

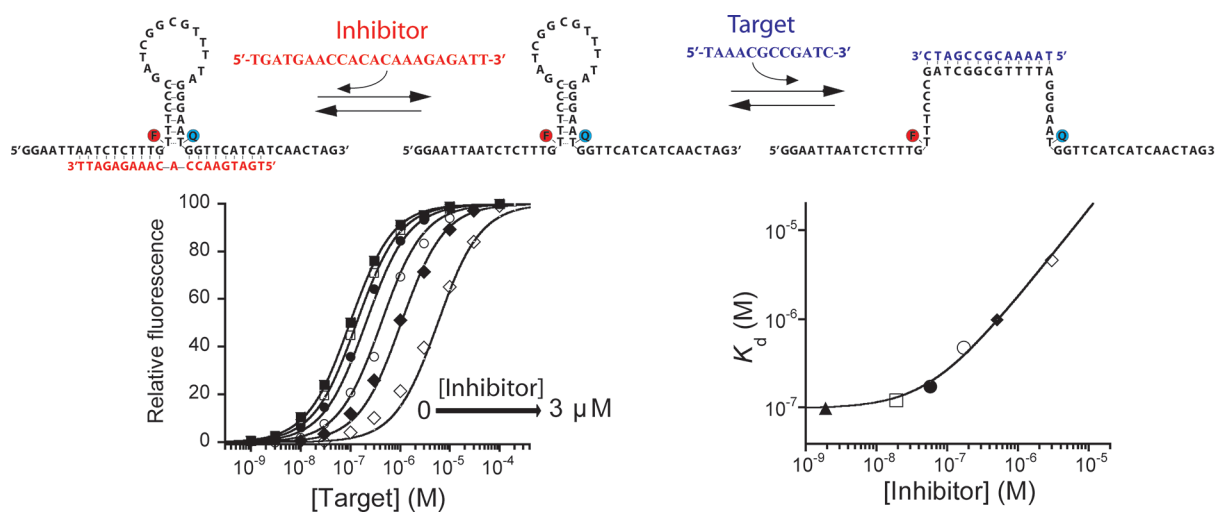


**Figure 2.** Rational design of an allosterically inhibited biosensor. (top) We engineered allosteric inhibition into a molecular beacon by adding two single-stranded “tails” that together serve as the allosteric binding site. The binding of an inhibitor to the two tails, bridging the junction between them, stabilizes the nonbinding state of the beacon, consequently reducing the target affinity and pushing the useful dynamic range to higher target concentrations. (bottom) As expected, the extent to which this allosteric inhibition shifted the dynamic range of the beacon (here and in all the experiments at 10 nM concentration) could be fine-tuned by varying the inhibitor concentration. Here we employed inhibitor concentrations producing (from left to right) 0, 5, 25, 50, 75, 90, and 98% occupancy of the allosteric site. Using the population-shift model (eqs 1 and 4) and the independently determined target and inhibitor affinities (Figure S1), we were able to simulate this allosteric behavior (solid curves) with high precision without the use of any floating parameters (see Figure S2 for details about the correlation between the estimated and experimentally observed values).

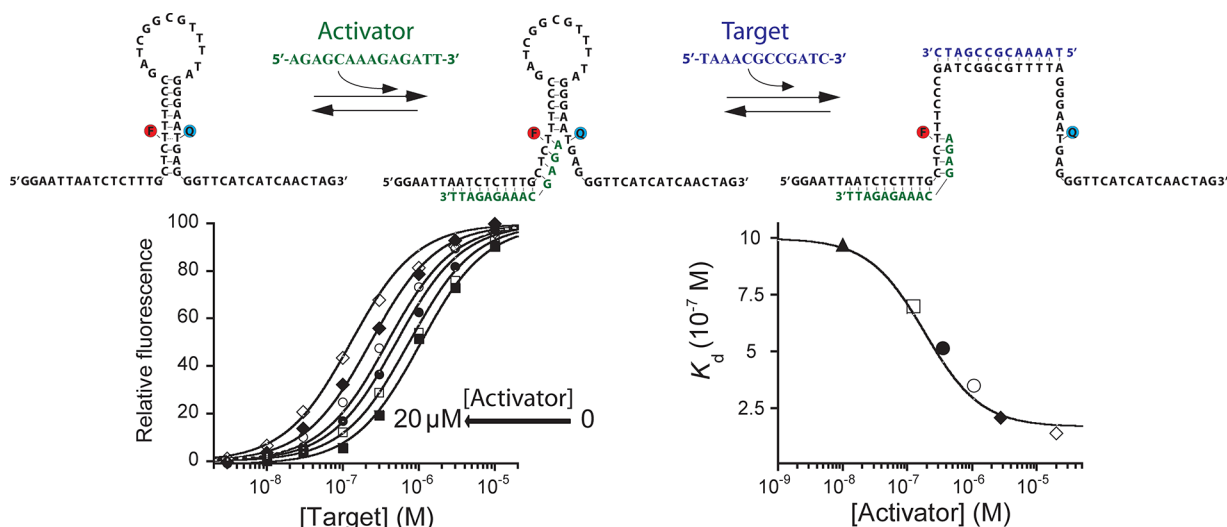


**Figure 3.** Rational design of an allosterically activated biosensor. (top) We engineered allosteric activation into a molecular beacon by using one single-stranded “tail” as an allosteric binding site. The activator sequence binding to this tail partially invades the stem, destabilizing the nonbinding state and thus improving the target affinity. (bottom) The extent of this activation could be fine-tuned by changing the activator concentration. Here we used concentrations producing (from right to left) 0, 2, 10, 25, 50, 75, and 95% occupancy of the allosteric site. Using the population-shift model (eqs 1 and 5) and the dissociation constants of the beacon for its target and the activator (Figure S4), we were able to simulate this allosteric behavior (solid curves) with high precision without the use of *any* adjustable parameters (see Figure S2 for details about the correlation between the simulated and experimentally observed values).

$$K_s(\text{inhib}) = K_s^0 \left( \frac{K_i}{K_i + [I]} \right) \quad (3)$$

where  $K_s^0$  is the switching equilibrium constant in the absence of inhibitor,  $K_i$  is the dissociation constant for binding of the inhibitor to the allosteric site of our modified molecular beacon, and  $[I]$  is the inhibitor concentration. The overall  $K_d$  of the molecular beacon thus becomes:

$$K_d(\text{inhib}) = K_d^{\text{int}} \left( \frac{1 + K_s^0 \left( \frac{K_i}{K_i + [I]} \right)}{K_s^0 \left( \frac{K_i}{K_i + [I]} \right)} \right) \quad (4)$$

We used previously employed methods<sup>12</sup> to determine  $K_d^{\text{int}}$  and  $K_s^0$  for this modified beacon. A small but detectable decrease in the beacon’s output associated with inhibitor binding (which brings the fluorophore and quencher into closer proximity) likewise provided an independent means of measuring  $K_i$  (Figure S1 in the Supporting Information). Using these values in eqs 1 and 4 we were able to simulate the output of our molecular beacon quantitatively over a range of target and inhibitor concentrations *without the use of any fitting parameters* (solid lines in Figure 2, bottom), highlighting the ability of the population-shift model to account for the behavior of this simple allosteric system at equilibrium (Figure S3).

The population-shift mechanism likewise provides a route for the design of sensors that can be activated allosterically using activators that destabilize the beacon’s nonbinding conformation, increasing  $K_s$ . We accomplished this using an oligonucleotide that binds to one tail of a “two-tailed” beacon in such a way that it partially invades the double-stranded stem, reducing its stability (Figure 3, top). An important distinction between activation and inhibition, however, is that activation cannot be carried out ad infinitum. Specifically, because the nonbinding conformation of the molecular beacon is dark, inhibitor binding can stabilize this state arbitrarily without increasing the

background fluorescence. In contrast, activators stabilize the emissive binding-competent state, thus increasing this background. For this reason, the extent to which an activator can improve the affinity of a receptor is limited, as excessive background fluorescence ultimately reduces the gain of the sensor (Figure S5). For this same reason, the “activatable” receptor we designed varied slightly from the receptor employed in the above inhibition studies. Specifically, we placed this construct’s fluorophore and quencher pair in the middle of a nine-base-pair stem and designed an activator that disrupts only four of these nine base pairs (Figure 3).<sup>16</sup>

The allosterically activated molecular beacon performed as expected. In the absence of its activator, the dose–response curve of the modified molecular beacon was well-described by the expected hyperbolic binding curve (eq 1) with a dissociation constant of 1.06  $\mu\text{M}$  (Figure 3). Upon the addition of activator, the sensor’s  $K_d$  decreased monotonically, reaching 0.12  $\mu\text{M}$  at 20  $\mu\text{M}$  activator. Confirming the validity of the population-shift model, the observed affinity was well-modeled (Figure S2) using eq 1 with  $K_d$  given by eq 5:

$$K_d(\text{act}) = K_d^{\text{int}} \left( \frac{1 + K_s^0}{K_s^0} \right) \left( \frac{1 + \frac{[A]}{K_{\text{act}}}}{1 + \frac{[A]}{\alpha K_{\text{act}}}} \right) \quad (5)$$

where  $K_{\text{act}}$  is the dissociation constant of the beacon/activator complex,  $\alpha$  is the ratio of the dissociation constants in the presence of saturating activator and the absence of activator, and  $[A]$  is the activator concentration.

A final important consideration is that the allosteric control presented here does not alter the target specificity. That is, because the allosteric binding site is separated from the target-binding element, our allosterically activated molecular beacon retains the same discrimination power (perfect match target vs a 1-base mismatch) as the unmodified parent beacon (Figure S7).

Here we have employed the population-shift model for rational engineering of allosteric regulation into a representative structure-switching biosensor over 3 orders of magnitude via the introduction of the appropriate concentration of allosteric inhibitor or activator. Consistent with the design principles we have employed, the input–output curves of both the inhibited and activated sensors were quantitatively described by the population-shift model, supporting our argument that this mechanism provides a convenient method by which finely tuned allostery can be introduced into structure-switching biosensors.

Because of their simple structure and easy “designability”, DNA molecular beacons are particularly amenable to the engineering approaches demonstrated here. This said, we believe that these approaches provide a route by which allosteric regulation can be introduced into many conformation-switching biosensors. Aptamer-based sensors, for example, can be inhibited via complementary sequences that stabilize double-stranded, non-target-binding states<sup>17</sup> and likely can be activated by sequences that suppress this effect (by sequestering the inhibitor). Even protein-based switches can be modulated via the population-shift mechanism. For example, we previously demonstrated the ease with which single-domain proteins can be re-engineered to support binding-induced folding.<sup>18</sup> We speculate that antibodies that bind a conformational epitope should be able to stabilize the native state of such a protein, thus activating it, while antibodies directed against epitopes exposed only in the unfolded state should, conversely, produce inhibition.

The availability of tunable biomolecules could prove to be of value in many biotechnologies. An obvious application, of course, is, as shown here, the development of sensors that circumvent the fixed dynamic ranges associated with traditional biomolecular recognition elements. More speculatively, the availability of tunable bioreceptors may be useful in the field of synthetic biology. The re-engineering of new cellular functions through the design of synthetic gene networks that can be fine-tuned through the use of allosteric effectors could provide a powerful tool for precise modulation of genetic regulatory networks, thus allowing their application in biomanufacturing.<sup>19</sup>

## ■ ASSOCIATED CONTENT

### Supporting Information

Supporting methods and figures. This material is available free of charge via the Internet at <http://pubs.acs.org>.

## ■ AUTHOR INFORMATION

### Corresponding Author

kwp@chem.ucsb.edu

### Present Address

<sup>¶</sup>Departement de Chimie, Université de Montréal, Montréal 235 Québec, Canada H3C 3J7.

### Author Contributions

<sup>#</sup>F.R. and A.V.-B. contributed equally.

### Notes

The authors declare no competing financial interest.

## ■ ACKNOWLEDGMENTS

The authors acknowledge members of our research group for helpful discussions on the manuscript. This work was supported by the NIH (Grant R01EB007689 to K.W.P.), the Fonds de Recherche du Québec Nature et Technologies

(FRQNT) (to A.V.-B.), the MIUR (FIRB “Futuro in Ricerca” to F.R.), the Bill & Melinda Gates Foundation through the Grand Challenges Exploration Initiative (OPPI061203 to F.R.) and the Marie Curie International Outgoing Fellowship within the 7th European Community Framework Programme (PIOFGA-2011-298491 to F.R.).

## ■ REFERENCES

- (1) Perutz, M. *Mechanisms of Cooperativity and Allosteric Regulation in Proteins*; Cambridge University Press: Cambridge, U.K., 1990.
- (2) (a) Goodey, N. M.; Benkovic, S. J. *Nat. Chem. Biol.* **2008**, *4*, 474. (b) Gunasekaran, K.; Ma, B.; Nussinov, R. *Proteins* **2004**, *57*, 433. (c) Tsai, C.; Del Sol, A.; Nussinov, R. *Mol. BioSyst.* **2009**, *5*, 207.
- (3) (a) Khalil, A. S.; Collins, J. J. *Nat. Rev. Genet.* **2010**, *11*, 367. (b) Purnick, P. E. M.; Weiss, R. *Nat. Rev. Mol. Cell Biol.* **2009**, *10*, 410. (c) Savage, D. F.; Way, J.; Silver, P. A. *ACS Chem. Biol.* **2008**, *3*, 13.
- (4) Yang, H.; Liu, H.; Kang, H.; Tan, W. *J. Am. Chem. Soc.* **2008**, *130*, 6320.
- (5) (a) Lubin, A. A.; Plaxco, K. W. *Acc. Chem. Res.* **2010**, *43*, 496. (b) Wang, J. *Anal. Chim. Acta* **2002**, *469*, 63.
- (6) (a) McDaniel, R.; Ebert-Khosla, S.; Hopwood, D. A.; Khosla, C. *Nature* **1995**, *375*, 549. (b) Soukup, G. A.; Breaker, R. R. *Proc. Natl. Acad. Sci. U.S.A.* **1999**, *96*, 3584. (c) Breaker, R. R. *Nature* **2004**, *432*, 838.
- (7) (a) Guntas, G.; Ostermeier, M. *J. Mol. Biol.* **2004**, *336*, 263. (b) Guntas, G.; Mansell, T. J.; Kim, J. R.; Ostermeier, M. *Proc. Natl. Acad. Sci. U.S.A.* **2005**, *102*, 11224.
- (8) (a) Choi, B.; Zocchi, G.; Canale, S.; Wu, Y.; Chan, S.; Perry, L. J. *Phys. Rev. Lett.* **2005**, *94*, No. 038103. (b) Choi, B.; Zocchi, G. *J. Am. Chem. Soc.* **2006**, *128*, 8541.
- (9) (a) Famulok, M.; Hartig, J. S.; Mayer, G. *Chem. Rev.* **2007**, *107*, 3715. (b) Zhang, D. Y.; Winfree, E. *J. Am. Chem. Soc.* **2008**, *130*, 13921.
- (10) Vallée-Bélisle, A.; Plaxco, K. W. *Curr. Opin. Struct. Biol.* **2010**, *20*, 518.
- (11) Plaxco, K. W.; Soh, H. T. *Trends Biotechnol.* **2011**, *29*, 1.
- (12) Vallée-Bélisle, A.; Ricci, F.; Plaxco, K. W. *Proc. Natl. Acad. Sci. U.S.A.* **2009**, *106*, 13802.
- (13) (a) Ma, B.; Kumar, S.; Tsai, C.; Nussinov, R. *Protein Eng.* **1999**, *12*, 713. (b) Ma, B.; Shatsky, M.; Wolfson, H. J.; Nussinov, R. *Protein Sci.* **2002**, *11*, 184. (c) Kumar, S.; Ma, B.; Tsai, C.; Sinha, N.; Nussinov, R. *Protein Sci.* **2000**, *9*, 10. (d) Tsai, C. J.; Ma, B.; Nussinov, R. *Proc. Natl. Acad. Sci. U.S.A.* **1999**, *96*, 9970.
- (14) (a) Ricci, F.; Vallée-Bélisle, A.; Plaxco, K. W. *PLoS Comput. Biol.* **2011**, *7*, No. e1002171. (b) Vallée-Bélisle, A.; Ricci, F.; Plaxco, K. W. *J. Am. Chem. Soc.* **2012**, *134*, 2876.
- (15) (a) Tyagi, S.; Kramer, F. R. *Nat. Biotechnol.* **1996**, *14*, 303. (b) Marras, S. A. E.; Tyagi, S.; Kramer, F. R. *Clin. Chim. Acta* **2006**, *363*, 48.
- (16) The stem length must be controlled to reduce the possibility of undesired dimerization of receptors. The raw fluorescence signals suggested that such dimerization did not occur under our experimental conditions (Figure S6).
- (17) White, R. J.; Rowe, A. A.; Plaxco, K. W. *Analyst* **2010**, *135*, 589.
- (18) Kohn, J. E.; Plaxco, K. W. *Proc. Natl. Acad. Sci. U.S.A.* **2005**, *102*, 10841.
- (19) (a) Babiskin, A. H.; Smolke, C. D. *Nucleic Acids Res.* **2011**, *39*, 5299. (b) Beisel, C. L.; Chen, Y. Y.; Culler, S. J.; Hoff, K. G.; Smolke, C. D. *Nucleic Acids Res.* **2011**, *39*, 2981.